

RESEARCH ARTICLE

Synthesis, Characterization, and Evaluation of Cytotoxic Effects of Novel Hybrid Steroidal Heterocycles as PEG Based Nanoparticles

Mervat M Abd Elhalim¹, Nasser S M Ismail², Shaymaa M M Yahya¹, Yasmin Y Omar¹, Ahmed A Abd Rabou¹, Deena S Lasheen³, Mahmoud F Zawrah⁴, Gamal A Elmegeed^{1*}

Abstract

Anticancer agents featuring hybrid molecules can improve effectiveness and diminish drug resistance. The current study aimed to introduce newly synthesized heterocyclic steroids of promising anticancer effects loaded in polyethylene glycol (PEG)-based nanoparticles form. Several heterocyclic steroids (1-9) were synthesized via multicomponent reactions (MCRs) and confirmed via the analytical and spectral data. Compounds 1, 2, 3, 4, 5, 6, 7 and 9, were investigated individually in their free and PEG based nano-size hybrid forms as anticancer agents against three human cell lines: hepatocellular carcinoma cells (HepG2); breast cancer cells (MCF-7); and colon cancer cells (HCT116). The neutral red supravital dye uptake assay was employed. Compound 6 in its PEG based nano-size form exhibited the best cytotoxic effects against HepG2 and HCT116 cell lines, with IC₅₀ values of 2.44 μmol/l and 2.59 μmol/l, respectively. In addition, it demonstrated a low IC₅₀ value against MCF-7 (3.46 μmol/l) cells. This study introduced promising anticancer agents acting through conversion into PEG-based nanoparticles.

Keywords: Cytotoxicity- Heterocycles- Multicomponent reactions- Nanoparticles- Steroids

Asian Pac J Cancer Prev, **18** (7), 1937-1946

Introduction

Cancer is a multicellular disease that can arise from any cell types and organs with a multi-factorial etiology (Hanahan and Weinberg 2000). It is the leading cause of death worldwide, accounting for 7.6 million deaths (around 13% of all deaths) in 2008 according to World health organization (WHO). In Cancer patients, chemotherapy is the only choice of treatment. Unfortunately, development of drug resistance in tumor after treatment is always a major obstacle to the successful management of cancer (Wu et al., 2006). Thus, developing new therapeutic agents that can overcome drug resistance becomes an urgent need for cancer patients.

Steroids have always attracted considerable attention because of being a fundamental class of biological signaling molecules. They can regulate a variety of biological processes, so they are considered good candidates for drug development in treatment of large number of diseases including cardiovascular (Dubey et al., 2002), autoimmune diseases (Latham et al., 2003), brain tumors, breast cancer, prostate cancer, osteoarthritis, etc.

(Sheridan et al., 1988). Presence of different functional groups located around the rigid tetracyclic core leads to diversity in the biological actions as these serve as substrates for different targets. In recent time a lot of attentions have been paid on structural modification of steroid compounds through incorporation of heteroatoms (Elmegeed et al., 2011; Zhang et al., 2013). These heteroatoms may be present in the main ring system or in the additional fused ring. The incorporation of different types of heteroatoms to steroid skeleton enhanced their various biological activities (Singh et al., 1991).

Multicomponent reactions (MCRs) are considered a superior method for the production of small-molecule compounds libraries and are indispensable for structure-activity relationship (SAR) studies. In a typical multicomponent process, more than two components are combined in a one reaction, thereby enrolling an operationally effective and highly modular way of the synthesis of structurally diverse molecular entities (Váradi et al., 2016). Recently several modified steroids were synthesized via MCRs (Mohareb et al., 2016).

Nanoparticles (NP) have been considered potent drug

¹Hormones Department, Medical Research Division, ⁴Center of Excellence for Advanced Sciences, Advanced Materials and Nanotechnology Group, National Research Centre, Dokki, ²Pharmaceutical Chemistry Department, Faculty of Pharmaceutical Sciences and Pharmaceutical Industries, Future University, ³Pharmaceutical Chemistry Department, Faculty of Pharmacy, Ain Shams University, Cairo, Egypt. *For Correspondence: gamalae@hotmail.com

vehicles due to their numerous important technological advantages, for instance, long half-life, high loading capacity (Ghosh et al., 2010). Also, NP are well known to concentrate mostly at cancer sites due to poor lymphatic drainage of macro-molecules in these sites and the enhanced permeability and retention effect (EPR) of cancer cells due to which the NP can pass through enlarged pores in the capillary endothelium pores of tumor cells (Lammers et al., 2008). Nanoparticles surface can be modified by using highly hydrophilic polymers, such as polyethyleneglycol (PEG) which are hydrophobic surfaces. The addition of PEG to the NP formulation increases the retention and circulation time by reducing uptake by opsonins in the Reticuloendothelial system (RES). It was reported previously that particles remained in rat circulation 40-times longer when coated than uncoated with PEG (Tan et al., 1993).

Our research group have many trials to develop facile and convenient route for the synthesis of steroid based compounds containing heteroatoms and screening their biological activities (Elmegeed et al., 2005; El-Far et al., 2009; Elmegeed et al., 2015). Encouraged by the preceding information, the goal of these investigations is to develop new drug candidates for cancer treatment. Steroidal heterocycles have been prepared via MCRs and converted to NP and tested in-vitro against liver, breast and colon cancer human cell lines.

Materials and Methods

Synthetic methods, analytical and spectral data

Starting steroid 5 α -cholestan-3-one, was purchased from Sigma Company, St. Louis, MO, USA. All solvents were anhydrous by distillation before its use. All melting points were measured using an Electrothermal apparatus and are uncorrected. The IR spectra were recorded in (KBr discs) on a shimadzu FT-IR 8201 PC spectrometer and expressed in cm⁻¹. The ¹H NMR and ¹³C NMR spectra were recorded with Jeol instrument (Japan), at 270 and 125 MHz respectively, in DMSO-d₆ as solvent and chemical shifts were recorded in ppm relative to TMS. The spin multiplicities were abbreviated by the letters: s-singlet, d-doublet, t-triplet, q-quartet and m (multiplet, more than quartet). Mass spectra were recorded on a GCMS-QP 1000 ex spectra mass spectrometer operating at 70 eV. Elemental analyses were carried by the Microanalytical Data Unit at the National Research Centre, Giza, Egypt and the Microanalytical Data Unit at Cairo University, Giza, Egypt. The reactions were monitored by thin layer chromatography (TLC) which was carried out using Merck 60 F254 aluminum sheets and visualized by UV light (254 nm). The mixtures were separated by preparative TLC and gravity chromatography. All steroid derivatives showed the characteristic spectral data of cyclopentanoperhydrophenanthrene nuclei of cholestane series were similar to those reported in literature (Gacs-Baitz et al., 1990).

General procedure for compounds 1 and 2

A mixture of 5 α -cholestan-3-one (0.38 g, 1mmol), p-methoxybenzaldehyde (0.13 g, 1mmol) and malononitrile

(0.06 g, 1mmol) in absolute ethanol (50 ml) containing ammonium acetate (0.98 g, 2% excess) or piperidine (1ml) was heated under reflux for 4-5 hours until all starting materials had disappeared as indicated by TLC. The reaction mixture was treated with ice/water mixture. The formed solid product, in each case, was collected by filtration and crystallized from absolute ethanol.

8-Amino-10-(4-methoxyphenyl)-11a, 13a-dimethyl-1-octyl-2, 3, 3a, 3b, 4, 5, 5a, 6, 6a, 7, 11, 11a, 11b, 12, 13, -13a-hexadecahydro-1H-cyclopenta[5,6]naphtho[1,2-g]quinoline-9-carbonitrile (1).

Yellow crystals, yield 0.48 g (85%); mp 105 -107 °C; IR (KBr, cm⁻¹): ν 3435-3350 (NH₂-NH), 2936, 2864 (CH-aliphatic), 1032 (CH-aromatic), 2211 (CN), 1566 (C=C). ¹H NMR (DMSO-d₆, ppm): δ = 0.84 (s, 3H, CH₃-19), 0.85 (d, 6H, 26-CH₃, 27-CH₃), 0.93 (d, 3H, 21-CH₃), 0.95 (s, 3H, CH₃), 1.09 (s, 3H, CH₃-18), 1.25-1.33 (m-6H, 3CH₂-aliphatic), 3.73 (s, 3H, OCH₃), 6.86 (s, 2H, NH₂, D₂O-exchangeable), 6.96 - 7.42 (m, 4H- aromatic-H). ¹³C NMR (DMSO-d₆-ppm): δ = 28.30 (C-1), 50.10 (C-3), 38.90 (C-4), 40.10 (C-5), 27.20 (C-6), 27.90 (C-7), 35.70 (C-8), 35.00 (C-9), 46.50 (C-10), 22.70 (C-11), 35.72 (C-12), 46.40 (C-13), 46.20 (C-14), 27.30 (C-15), 29.80 (C-16), 47.90 (C-17), 20.40 (C-18), 21.10 (C-19), 115.90 (CN), 131.60, 139.90 (C=C), 19.4, 23.2, 23.2 (CH₃-aliphatic), 36.10, 24.60, 39.30 (CH₂-aliphatic), 35.80, 28.10 (CH-aliphatic), 56.10 (C-OCH₃), 113.90, 128.20, 127.40, 159.20, 143.50 (C-aromatic). MS (EI): m/z (%): 570 (M⁺+1, 60), 462 (8), 344 (8), 225 (9), 81 (40), 64 (80). Calc for C₃₈H₅₅N₃O (569.863): C, 79.95; H, 9.61; N, 7.56, found: C, 80.06; H, 9.53; N, 7.25 %.

8-Amino-10-(4-methoxyphenyl)-11a, 13a-dimethyl-1-octyl-1, 2, 3, 3a, 3b, 4, 5, 5a, 6, 6a, 11, 11a, 11b, 12, 13, -13a-hexadecahydrocyclopenta[5,6]naphtho[1,2-g]-chromene-9-carbonitrile (2).

Dark orange crystals, yield 0.43 g (76%); mp 77-80 °C; IR (KBr, cm⁻¹): ν 3452-3350 (NH₂-NH), (NH₂), 2934, 2865 (CH-aliphatic), 2217 (CN), 1604 (C=C). ¹H NMR (DMSO-d₆, ppm): δ = 0.82 (s, 3H, CH₃-19), 0.85 (d, 6H, 26-CH₃, 27-CH₃), 0.93 (d, 3H, 21-CH₃), 1.18 (s, 3H, CH₃-18), 1.25-1.33 (m-6H, 3CH₂-aliphatic), 3.74 (s, 3H, OCH₃), 4.20 (s, 1H, pyrane), 6.34 (s, 2H, NH₂, D₂O-exchangeable), 6.84-7.11 (m, 4H- aromatic-H). ¹³C NMR (DMSO, ppm): δ = 27.20 (C-1), 53.80 (C-3), 35.90 (C-4), 40.10 (C-5), 27.20 (C-6), 27.90 (C-7), 35.70 (C-8), 35.00 (C-9), 46.50 (C-10), 22.70 (C-11), 35.72 (C-12), 46.40 (C-13), 46.20 (C-14), 27.30 (C-15), 29.80 (C-16), 47.90 (C-17), 20.40 (C-18), 21.10 (C-19), 115.90 (CN), 131.6, 139.9 (C=C), 19.40, 23.20, 23.20 (CH₃-aliphatic), 36.10, 24.60, 39.30 (CH₂-aliphatic), 35.80, 28.10 (CH-aliphatic), 56.10 (C-OCH₃), 114.20, 127.40, 159.90 (C-aromatic). MS (EI): m/z (%): 570 (M⁺, 66), 517 (40), 80 (35), 64 (100). Calc for C₃₈H₅₄N₂O₂ (570.848): C, 79.81; H, 9.41; N, 5.03, found: C, 79.72; H, 9.39; N, 5.10 %.

Synthetic procedure for compounds 3

12-(4-Methoxyphenyl)-13a, 15a-dimethyl-1-octyl-10-phenyl-1, 2, 3, 3a, 3b, 4, 5, 5a, 6, 6a, 7, 10, 13, 13a, -13b, 14, 15, 15a-octadecahydro-11H-cyclopenta[5,6]naphtho[1,2-g]pyrimido[4,5-b]quinolin-11-imine (3).

To a 1mmol from compound 1 (0.57 g) in absolute ethanol (30 ml), 1 ml glacial acetic acid was added, and equimolar amount of aniline (0.09 g, 1 mmol). The reaction mixture was heated under reflux about 2-3 hr until all starting materials had disappeared as indicated by TLC. The reaction mixture was neutralized with sodium bicarbonate, the formed solid product was collected by filtration, dried and crystallized from ethanol (95%).

Pale yellow crystals, yield 0.60 g (90%); mp 100-103 °C; IR (KBr, cm⁻¹): ν 3293 (NH), 2926, 2857 (CH-aliphatic), 1600 (C=C). ¹HNMR (DMSO-d₆, ppm): δ = 0.85 (d, 6H, 26-CH₃, 27-CH₃), 0.87 (s, 3H, CH₃-19), 0.93 (d, 3H, 21-CH₃), 1.25- 1.33 (m-6H, 3CH₂-aliphatic), 1.90 (s, 3H, CH₃-18), 3.33 (s, 3H, OCH₃), 6.90-7.50(m, 9H, aromatic), 9.90 (s, 1H, NH exchangeable). ¹³CNMR (DMSO, ppm): δ =34.80 (C-1), 54.60 (C-3), 36.70 (C-4), 38.80 (C-5), 25.20 (C-6), 27.90 (C-7), 35.70 (C-8), 43.20 (C-9), 46.50 (C-10), 22.70 (C-11), 35.72 (C-12), 46.40 (C-13), 46.20 (C-14), 27.30 (C-15), 29.80 (C-16), 47.90 (C-17), 20.40 (C-18), 21.10 (C-19), 96.10, 145.50, 146.80, 158.90 (C-pyrimidine), 131.60, 139.90 (C=C), 19.40, 23.20, 23.20 (CH₃-aliphatic), 36.10, 24.60, 39.30 (CH₂-aliphatic), 35.80, 28.10 (CH-aliphatic), 56.10 (C-OCH₃), 114.20, 127.40, 159.90 (C-aromatic). MS (EI): m/z(%): 673 (M⁺+1, 20), 567 (48), 477 (28), 108 (7). Calc for C₄₅H₆₀N₄O (672.480): C, 80.00; H, 9.26; N, 8.30%, found: C, 80.2; H, 9.52; N, 8.42%.

General procedure for compounds 4 and 5

To a mixture of compound 1 (0.57 g, 1 mmol) and hydrazine hydrate 98% (0.05 g, 1 mmol) or phenyl hydrazine (0.10 g, 1mmol) in absolute ethanol (30 ml), 1ml of triethylamine was added. The reaction mixture was heated under reflux about 3-5 hours, the reaction mixture was monitored by TLC, after complete disappearance of the reactant, the solvent was evaporated under reduced pressure and the residue oil was solidified by boiling in the petroleum ether. The result product was purified with appropriate solvent.

11-(4-Methoxyphenyl)-12a, 14a-dimethyl-1-octyl-1, 2, 3, 3a, 3b, 4, 5, 5a, 6, 6a, 8, 9, 12, 12a, 12b, 13, 14, 14a-octadecahydrocyclopenta[5,6]naphtho[1,2-g]pyrazolo[3,4-b]quinolin-10(10aH)-imine (4).

White yellowish crystals from absolute ethanol, yield 0.23 g (40%); mp 93- 95 °C; IR (KBr, cm⁻¹): ν 3409 (NH), 2932, 2867 (CH-aliphatic), 1567 (C=C). ¹H NMR (DMSO-d₆, ppm): δ = 0.76 (s, 3H, CH₃-19), 0.85 (d, 6H, 26-CH₃, 27-CH₃), 0.93 (d, 3H, 21-CH₃), 1.16 (s, 3H, CH₃-18), 1.25-1.33 (m-6H, 3CH₂-aliphatic), 3.70 (s, 3H, OCH₃), 6.45-7.18 (m, 6H, aromatic and NH). ¹³CNMR (DMSO, ppm): δ =34.80 (C-1), 58.10 (C-3), 35.70 (C-4), 38.80 (C-5), 25.20 (C-6), 27.90 (C-7), 35.70 (C-8), 43.20(C-9), 46.50 (C-10), 22.70 (C-11), 35.72 (C-12), 46.40 (C-13), 46.20 (C-14), 27.30 (C-15), 29.80 (C-16), 47.90 (C-17), 20.80 (C-18), 21.10 (C-19), 127.60, 139.90 (C=C), 19.40, 23.20, 23.20 (CH₃-aliphatic), 36.10, 24.60, 39.30 (CH₂-aliphatic), 35.80, 28.10 (CH-aliphatic), 56.10 (C-OCH₃), 114.20, 127.40, 159.90 (C-aromatic). MS (EI): m/z (%): 585 (M⁺+1, 70), 527 (16), 502 (16), 80 (23), 64 (94). Calc for C₃₈H₅₆N₄O (584.880): C, 78.03; H, 9.65; N, 9.58, found: C, 78.18; H, 9.37; N, 9.49 %.

11-(4-Methoxyphenyl)-12a,14a-dimethyl-1-octyl-9-phenyl, 2, 3, 3a, 3b, 4, 5, 5a, 6, 6a, 8, 9, 12, 12a, -12b, 13, -14, 14a-octadecahydrocyclopenta[5,6]naphtho[1,2-g]pyrazolo[3,4-b]quinolin-10(10aH)-imine (5).

Pale brown crystals from absolute ethanol, yield 0.43 g (66%); mp 85-87 °C; IR (KBr, cm⁻¹): ν 3424 (NH), 2936, 2864 (CH-aliphatic), 1565 (C=C). ¹HNMR (DMSO-d₆, ppm): δ = 0.78 (s, 3H, CH₃-19), 0.85 (d, 6H, 26-CH₃, 27-CH₃), 0.93 (d, 3H, 21-CH₃), 1.15 (s, 3H, CH₃-18), 1.25-1.33 (m-6H, 3CH₂-aliphatic), 3.73 (s, 3H, OCH₃), 6.99-7.80 (m, 11H aromatic hydrogen and 2NH). ¹³CNMR (DMSO, ppm): δ =34.80 (C-1), 58.70 (C-3), 35.70 (C-4), 38.80 (C-5), 25.20 (C-6), 27.90 (C-7), 35.70 (C-8), 43.20 (C-9), 46.50 (C-10), 22.70 (C-11), 35.72 (C-12), 46.40 (C-13), 46.20 (C-14), 27.30 (C-15), 29.80 (C-16), 47.90 (C-17), 20.80 (C-18), 21.10 (C-19), 127.60, 139.90 (C=C), 19.40, 23.20, 23.20 (CH₃ aliphatic), 36.10, 24.60, 39.30 (CH₂-aliphatic), 35.80, 28.10 (CH-aliphatic), 56.10 (C-OCH₃), 114.20, 127.40, 159.90 (C-aromatic). MS (EI): m/z (%): 661 (M⁺+1, 10), 647 (7), 567 (20), 80 (23), 64 (94). Calc for C₄₄H₆₀N₄O (660.48): C, 79.95; H, 9.15; N, 8.48, found: C, 79.87; H, 9.30; N, 8.32%.

General procedure for compounds 6 and 7

To a suspension of compound 1 (0.57 g, 1mmol) in freshly prepared sodium ethoxide, equimolar amount of urea (0.06 g, 1 mmol) or thiourea (0.07 g, 1 mmol) in absolute ethanol was added dropwise with stirring. After that the reaction mixture was heated under reflux for 3-5 hr until the starting materials had disappeared as indicated by TLC. The solvent was evaporated under vacuum and the remaining solids were treated with ethanol (70%) and the result powder was crystallized from proper solvent.

11-Imino-12-(4-methoxyphenyl)-13a, 15a-dimethyl-1-octyl-3, 3a, 3b, 4, 5, 5a, 6, 6a, 8, 10, 11, 11a, 13, -13a, 13b, 14, 15, 15a-octadecahydro-1H-cyclopenta[5,6]naphtho[1,2-g]pyrimido[4,5-b]quinoline-9(2H)-thione (6).

White crystals from absolute ethanol, yield 0.34 g (55%), mp 95-97°C; IR (KBr, cm⁻¹): ν 3404 (3NH), 2935, 2867 (CH-aliphatic), 1575 (C=C), 1608 (C=N), 1175 (C=S). ¹HNMR (DMSO-d₆, ppm): δ = 0.85 (d, 6H, 26-CH₃, 27-CH₃), 0.93 (d, 3H, 21-CH₃), 0.95 (s, 3H, CH₃-19), 1.23 (s, 3H, CH₃-18), 1.25-1.33 (m-6H, 3CH₂-aliphatic), 3.73 (s, 3H, OCH₃), 6.88-7.4 (m, 4H- aromatic-H). 8.65 (s, H, NH, D₂O-exchangeable), 9.51 (s, 2H, 2NH, D₂O-exchangeable). ¹³CNMR (DMSO-d₆-ppm): δ =34.10 (C-1), 53.10 (C-3), 33.20 (C-4), 37.20 (C-5), 25.30 (C-6), 25.80 (C-7), 34.70 (C-8), 42.90 (C-9), 44.10 (C-10), 20.80 (C-11), 31.40 (C-12), 43.80 (C-13), 46.00 (C-14), 21.20 (C-15), 23.70 (C-16), 42.90 (C-17), 20.30 (C-18), 20.80 (C-19), 44.00, 156.40, 178.20 (C-pyrimidine), 19.40, 23.20, 23.20 (CH₃-aliphatic), 36.10, 24.60, 39.30 (CH₂-aliphatic), 35.80, 28.10 (CH-aliphatic), 164.60 (C=N), 56.00 (C-OCH₃), 186.00 (C=S), 114.00, 127.20, 161.20 (C-aromatic). MS (EI): m/z (%): 628 (M⁺, 60), 616 (17), 598 (14), 528 (15), 80 (29), 64 (97). Calc for C₃₉H₅₆N₄OS (628.953): C, 74.48; H, 8.97; N, 8.91; S, 5.10, found: C, 74.34; H, 8.85; N, 8.72; S, 5.03%.

11-Imino-12-(4-methoxyphenyl)-13a, 15a-dimethyl-1-octyl-3, 3a, 3b, 4, 5, 5a, 6, 6a, 8, 10, 11, 11a, -13, 13a,

13b, 14, 15, 15a-octadecahydro-1H-cyclopenta[5,6] naphtho [1,2-g] pyrimido [4,5-b] quinolin-9 (2H)-one (7).

White crystals from absolute ethanol, yield 0.30g (50%), mp 95-96 °C; IR (KBr, cm⁻¹): ν 3387 (3NH), 2932, 2866 (CH-aliphatic), 1672 (C=O), 1574 (C=C), 1608 (C=N). ¹H NMR (DMSO-d₆, ppm): δ= 0.85 (d, 6H, 26-CH₃, 27-CH₃), 0.92 (s, 3H, CH₃-19), 0.93 (d, 3H, 21-CH₃), 1.23 (s, 3H, CH₃-18), 1.25-1.33 (m-6H, 3CH₂-aliphatic), 3.73 (s, 3H, OCH₃), 6.44-7.40 (m, 7H-aromatic-H and 3NH). ¹³CNMR (DMSO-d₆-ppm): δ=34.40 (C-1), 58.20 (C-3), 35.10 (C-2), 33.20 (C-4), 37.20 (C-5), 25.20 (C-6), 25.80 (C-7), 29.60 (C-8), 42.90 (C-9), 35.40 (C-10), 20.80 (C-11), 31.40 (C-12), 42.90 (C-13), 46.20 (C-14), 21.20 (C-15), 23.70 (C-16), 43.80 (C-17), 20.00 (C-18), 20.40 (C-19), 44.30, 154.40, 156.40 (C-pyrimidine), 19.40, 23.20, 23.20 (CH₃-aliphatic), 36.10, 24.60, 39.30 (CH₂-aliphatic), 35.80, 28.10 (CH-aliphatic), 56.20 (C-OCH₃), 162.00 (C=O), 114.00, 127.20, 161.20 (C-aromatic). MS (EI): m/z (%): 612 (M⁺, 70), 502 (26), 383 (7), 255 (45). Calc for C₃₉H₅₆N₄O₂ (612.888): C, 76.43; H, 9.21; N, 9.14, found: C, 76.70; H, 9.35; N, 9.32%.

General procedure for compounds 8 and 9

To a solution of compound 1 (0.57 g, 1mmol) in 15 ml potassium ethoxide (10%), carbon disulfide (1 mmol, 0.07 g) was added for the synthesis of compound 8 and excess (0.21 g) for the synthesis of compound 9 was added. the reaction mixture was heated under reflux for 4 hours until all starting materials had disappeared as indicated by TLC. The solvent was evaporated under vacuum and the remaining oil was treated with ice/water mixture and neutralized with dilute HCL. The obtained solid product was collected by filtration, dried, and crystallized from absolute ethanol.

12-(4-Methoxyphenyl)-13a, 15a-dimethyl-1-octyl-9-thioxo-3, 3a, 3b, 4, 5, 5a, 6, 6a, 8, 9, 10, -11a, 13, 13a, -13b, 14, 15, 15a-octadecahydro-1H-cyclopenta [5,6] naphtho [1,2-g] pyrimido [4,5-b] quinolin-11 (2H)-one (8).

Yellow crystals, yield 0.50 g (80%), mp 93-95 °C; IR (KBr, cm⁻¹): ν 3423 (NH), 2932, 2866 (CH-aliphatic), 1611 (C=O), 1567 (C=C), 1175 (C=S). ¹HNMR (DMSO-d₆, ppm): δ= 0.85 (d, 6H, 26-CH₃, 27-CH₃), 0.93 (d, 3H, 21-CH₃), 0.96 (s, 3H, CH₃-19), 1.29 (s, 3H, CH₃-18), 1.25-1.33 (m-6H, 3CH₂-aliphatic), 3.79 (m, 3H, OCH₃), 7.05-7.18 (m, 6H, aromatic hydrogen and 2NH). ¹³CNMR (DMSO-d₆-ppm): δ=34.00 (C-1), 34.40 (C-2), 35.20 (C-3), 33.20 (C-4), 37.20 (C-5), 25.30 (C-6), 25.80 (C-7), 29.60 (C-8), 42.90 (C-9), 35.40 (C-10), 20.80 (C-11), 31.40 (C-12), 42.90 (C-13), 46.00 (C-14), 21.20 (C-15), 23.20 (C-16), 43.80 (C-17), 20.20 (C-18), 20.50 (C-19), 48.80, 156.40, 172.70, 175.20 (C-pyrimidine), 19.40, 23.20, 23.20 (CH₃-aliphatic), 36.10, 24.60, 39.30 (CH₂-aliphatic), 35.80, 28.10 (CH-aliphatic), 183.00 (C=S), 167.60 (C=O), 56.10 (C-OCH₃), 127.00, 114.00, 161.00 (C-aromatic). MS (EI): m/z (%): 630 (M⁺+1, 70), 615 (17), 585 (12), 542 (4), 80 (26), 64 (97). Calc for C₃₉H₅₅N₃O₂S (629.401): C, 74.10; H, 8.67; N, 6.82; S, 5.21, found: C, 74.28; H, 8.50; N, 6.72; S, 5.32 %.

12-(4-Methoxyphenyl)-13a, 15a-dimethyl-1-octyl-3, 3a, 3b, 4, 5, 5a, 6, 6a, 10, 11a, 13, 13a, 13b, 14, 15,

15a-hexadecahydro-1H-cyclopenta [5,6] naphtho [1,2-g] pyrimido [4,5-b] quinoline-9,11 (2H,8H)-dithione (9).

Dark yellow crystals from absolute ethanol, yield 0.45 g (70%), mp 95 °C; IR (KBr, cm⁻¹): ν 3402 (2NH), 2934, 2867 (CH-aliphatic), 1574 (C=C), 1608 (C=N), 1248, 1175 (2C=S). ¹HNMR (DMSO-d₆, ppm): δ= 0.85 (d, 6H, 26-CH₃, 27-CH₃), 0.93 (d, 3H, 21-CH₃), 0.96 (s, 3H, CH₃-19), 1.29 (s, 3H, CH₃-18), 1.25-1.33 (m-6H, 3CH₂-aliphatic), 3.74 (s, 3H, OCH₃), 6.99-7.42 (m, 6H, aromatic hydrogen and 2H, NH). ¹³CNMR (DMSO-d₆, ppm): δ=35.0 (C-1), 35.10 (C-3), 33.20 (C-4), 37.20 (C-5), 25.30 (C-6), 25.80 (C-7), 29.60 (C-8), 42.90 (C-9), 35.40 (C-10), 20.80 (C-11), 31.40 (C-12), 42.90 (C-13), 46.00 (C-14), 21.20 (C-15), 23.20 (C-16), 43.80 (C-17), 20.20 (C-18), 20.50 (C-19), 75.50, 130.40, 186.30, 194.00 (C-pyrimidine), 19.40, 23.20, 23.20 (CH₃-aliphatic), 36.10, 24.60, 39.30 (CH₂-aliphatic), 35.80, 28.10 (CH-aliphatic), 186.30 (C=S), 56.10 (C-OCH₃), 114.00, 127.20 (C-aromatic). MS (EI): m/z (%): 645 (M⁺-1, 43), 585 (14), 542 (20), 276 (28), 80 (26), 64 (97). Calc for C₃₉H₅₅N₃OS₂ (646.004): C, 72.22; H, 8.45; N, 6.65; S, 10.15, found: C, 72.50; H, 8.39; N, 6.51; S, 10.32 %.

Preparation of PEG-based Nanoparticles

PEG-based nanoparticles, namely PEG-based cholestane heterocyclic derivatives nano emulsions (N1-N9), were synthesized using precipitation method (Vaculikova et al., 2012). Briefly, 2 ml Tween 80, 0.1 g sodium dodecyl sulfate (SDS), 0.3 g polyethylene glycol (PEG-macrogol 6,000), 0.5g sodium carboxy methyl cellulose (SCMC) and 1 g sodium carboxy methyl dextran (SCMD) were used as excipients. The excipients were dissolved in 10ml deionized water. The aqueous solutions of excipients were stirred for 10 min at 35 °C and 600 rpm. 0.04 g of each one of cholestane heterocyclic derivatives was dissolved in 2ml absolute ethanol; i.e., 2% solutions were prepared. The prepared solutions of the cholestane derivatives in ethanol were slowly dropped (2 ml) to the aqueous solutions (10 ml) of excipients. Then the system was stirred for 30 min and sonicated in ultrasonic water bath for 40 min as described in (Vaculikova et al., 2012).

Characterization of PEG-based Nanoparticles

The particle size distribution and zeta potential of the synthesized nanosized cholestane heterocyclic derivatives (N1-N9) were measured by Malvern Zetasizer system (Malvern Instruments, Westborough, Massachusetts). In Zetasizer, 1ml of the nanoparticles solution was filled in the disposable transparent sizing clear cuvette and sample was analyzed at 25 °C. The morphology and particle size of synthesized nanosized (N1-N9) were evaluated by Transmission Electron Microscope (TEM).

Dialysis of PEG-based Nanoparticles and entrapment efficiency measurement

Sample preparation for injection onto HPLC

Each PEG-loaded NP (0.1 ml) was diluted to 1ml and further diluted twice (1:10) with methanol. 50 µl was injected and drug content was determined by the reported High performance liquid chromatography (HPLC) method (Dueland et al., 1982).

HPLC condition

HPLC system Agilent1100 series with Quat pump a SPD-20A UV Visible variable wavelength detector set at 254 with deuterium lamp, and a 250 x 4.6 mm, 5 μ , C-18 reverse phase analytical column was used to determine total drug content and entrapment efficiency of the formulations. The mobile phase consisted of acetonitrile/ultrapure water 65/35 (v/v) was eluted at a flow rate 1 ml/min. Serial dilutions of standard were injected onto HPLC and their peak areas were determined. A linear standard curve was constructed by plotting peak areas versus the corresponding concentrations, the concentrations in samples were obtained from the standard curve.

The drug entrapment efficiency (EE) was calculated from the ratio of amount of drug obtained by HPLC (drug content in the synthesized PEG-based nanoparticles) to the total added starting amount of drug (0.04 g). Entrapment efficiency of drugs was determined by filtering a known amount of drug-loaded nanoparticles through a 10K MWCO filter dialysis membrane (Amicon, Millipore, Schwalbach, D) to separate the free drug.

In-vitro Cytotoxic Assay

Cell propagation and maintenance

Hepatocellular carcinoma cells HepG2, breast cancer cells MCF-7 and colon cancer cells HCT116 were purchased from American Type Culture Collection (ATCC), and maintained under the proper conditions. The cells were cultured in Dulbecco's modified Eagle's medium (Sigma-Aldrich, St Louis, Missouri, USA) supplemented with 100 IU/ml penicillin G sodium, 100 IU/ml streptomycin sulfate, 1% l-glutamine, and 10% fetal bovine serum at 37 °C in a humidified incubator with 5% CO₂. The cells were harvested after trypsinization (0.025% trypsin and 0.02% Ethylenediaminetetraacetic acid (EDTA) and washed twice with Dulbecco's phosphate-buffered saline (DPBS) (Bio-Whittaker, Lonza, Verviers, Belgium). When the cell density reached ~80%, cells were splitted for further culture. The experiments were conducted when the cells were in the logarithmic growth phase.

Cytotoxicity Assay

Cell viability was measured using a neutral red uptake assay (Repetto et al., 2008). The neutral red uptake assay provides a quantitative estimation of the number of viable cells in a culture. It is based on the ability of viable cells to incorporate and bind the supravital dye neutral red in the lysosomes. The cells were incubated with various concentrations of the tested compounds (6.25, 12.5, 25, 50 μ mol/l) for 48 h at a cell density of 10⁴ cells/well of a 96-well plate. A neutral red working solution (0.4 μ g/ml) (Sigma-Aldrich) was incubated overnight at 37°C in the same manner as the treated cells. In each well of the incubated cells, culture media were removed and neutral red medium (100 μ l) was added, and then incubated for 2 h to allow for vital dye incorporation into living cells. The neutral red media were removed and rinsed rapidly with Dulbecco's PBS buffer (150 μ l). Dye was extracted from the cells by adding extraction buffer [150 μ l, 1% acetic acid: 50% ethanol (96%): 49% deionized H₂O],

followed by rapid agitation for at least 10 min on a micrometer plate shaker. The extract neutral red color intensity was measured at 530 and 645 nm as excitation and emission wavelengths in a micro-titer plate reader spectrophotometer (Sorin, Biomedica S.p.A., Milan, Italy). Using the relation between log concentrations used and the neutral red intensity value, the IC₅₀ of the tested compounds were calculated. For the untreated cells (negative control), medium was added instead of the test compounds. A positive control Adrinamycin (doxorubicin) (Mr = 579.9) for HepG2, Cisplatin (Mr = 300.05) for HCT116, and Tamoxifen (Mr = 371.51) for MCF-7 were used as a cytotoxic natural agents yielding 100% inhibition. Dimethyl sulfoxide (DMSO) was the vehicle used for dissolution of the tested compounds and its final concentration on the cells was less than 0.2%. All tests and analyses were carried out in triplicate and the results were averaged.

Molecular Docking Study

Molecular modeling study was initiated in order to interpret the biological results and to determine further information about the binding orientations of the tested compounds and optimize a reliable model for predicting novel effective anti-tumor hits. Docking study was carried out for the target compounds into protein tyrosine kinase (PTK) using Discovery Studio 2.5 software (Accelrys Inc., San Diego, CA, USA). The docking study of the newly hybrid synthesized compounds was carried out, which were docked within the protein tyrosine kinase (PDB code: 1t46) (Shrestha et al., 2008). Interactive docking using C-DOCKER protocol was carried out for all the conformers of each compound of the tested set (1-9) to the selected active site, after energy minimization using prepared ligand protocol. Protein structure was prepared and the invalid or missing residues were added (Accelrys Inc., 2003). Re-docking lead compound with the same binding site showed docking energy = - 48 kcal/mol with small RMSD (0.909A) deviation in comparison to its crystal structure (Figure 1). The small RMSD values proved the validity of the used docking processes (Johnson et al., 2002). Each docked compound was assigned a score according to its binding mode onto the binding site (Vulpetti et al., 2005). In the study, the lead compound (STI-571) [4-[(4-methylpiperazin-1-yl)methyl]-N-[4-methyl-3-[(4-pyridin-3-yl)pyrimidin-2-yl]amino]-phenyl]-benzamide, commonly known as Imatinib or Gleevec was docked into its C-kit receptor PTK (PDB code: 1t46). It was found that the steroids derivatives were favorably fitted into the binding pocket of PTK which was comparable with the native ligand. Therefore, the STI-571 was selected as a reference ligand for the comparative study of binding action of the synthesized compounds in this study.

Results

Chemistry

One pot multicomponent reactions were attempted as a straight forward method for the synthesis of

Table 1. Particle Size, Zeta Potential and Determined Concentration of the Prepared PEG-Based Nanoparticles

Formulation code	Size (nm)	Zeta potential (mV)	HPLC/Conc. ($\mu\text{g/ml}$)
N1	22.25	-19.3	81.7
N2	25.94	-27.4	760.0
N3	7.63	-35.2	25.3
N4	2.85	-35.8	633.0
N5	20.5	-32.1	156.8
N6	60.88	-30.5	348.0
N7	227.90	-34.7	348.0
N8	15.79	-26.2	0.0
N9	18.37	-28.8	867.0

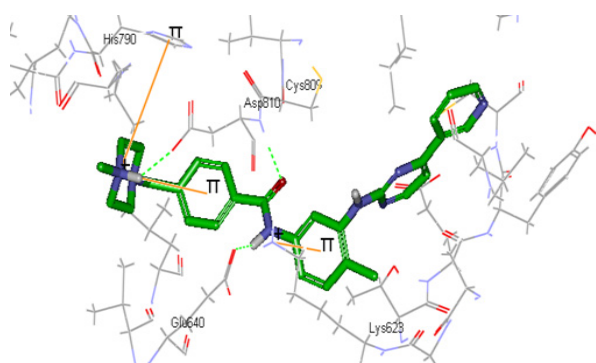


Figure 1. Validation of Accuracy and Performance of the Docking Algorithm (C-DOCKER). The docked STI ligand nearly superimposed on the native STI ligand exhibiting same number of hydrogen bonds with same amino acids involved by the native one

heterocyclic steroids. A mixture of 5α -cholestane-3-one, p-methoxybenzaldehyde and malononitrile was heated under reflux for 5 hours in absolute ethanol containing a catalytic amount of piperidine to afford the corresponding aminocholestanopyran derivative 2 (scheme 1). The formation of pyran derivative 2 can be explained by the possible mechanism represented in scheme 2. The reaction occur via initial formation of the intermediate acrylonitrile A followed by its nucleophilic attack of the anion of cholestanone to produce the intermediate B. The final product D was formed via the initial cyclization and subsequent tautomerization of the cyclic intermediate C. To survey the scope of this reaction for the synthesis of pyran and pyridine derivatives, different catalysts were used, thus the multicomponent reactions of cholestanone with malononitrile and p-methoxybenzaldehyde in absolute ethanol containing catalytic amount of ammonium acetate gave the aminocholestanopyridine derivative 1 (scheme1). All microanalytical and spectroscopic data were in accordance with the suggested compounds 1 and 2 (c.f. Materials and Methods).

The aminocholestanopyridine adduct 1 was allowed to react with aniline in glacial acetic acid to afford the corresponding cholestanopyridopyrimidine derivative 3 (scheme 3). On the other hand the reaction of compound 1 with hydrazine hydrate or phenyl hydrazine in absolute

Table 2. *In-Vitro* Cytotoxic Activity of the Newly Synthesized PEG Based Nanoparticles Compounds on the HepG2, MCF-7, HCT116 Cancer Cell Line

Compound /Cell line	IC ₅₀ (mmol/l)		
	HepG2	MCF-7	HCT116
N1	8.51	2.45	26.3
N2	40.73	41.6	48.9
N3	8.31	2.45	3.21
N4	42.6	2.88	10.11
N5	25.5	31.6	37.1
N6	2.44	3.46	2.59
N7	12.02	3.09	17.3
N9	50	3.08	10.09
Reference drug	Doxorubicin = 2.63	Tamoxifen = 3.09	Cisplatin = 4.67

ethanol containing a catalytic amount of triethylamine afforded the corresponding cholestanopyridopyrazole derivatives 4 or 5 respectively (scheme 3). For more utility of the pervious method to synthesize different active heterocyclic steroids, urea and thiourea were used. The reaction of aminocholestanopyridine derivative 1 with equimolar amount of urea or thiourea in freshly prepared sodium ethoxide afforded the corresponding cholestanopyridopyrimidine derivatives 6 or 7 respectively (scheme 4).

Aminocholestanopyridine derivative 1 was allowed to react with equimolar amount of carbon disulfide in alcoholic potassium hydroxide solution (10%) to form the corresponding cholestanopyridopyrimidine-thione derivative 8 (scheme 5). Meanwhile, carrying out the pervious reaction in the presence of excess of carbon disulfide afforded the cholestanopyridopyrimidine-dithione derivative 9 (scheme 5). Analytical and spectral data of all products were consistent with their respective

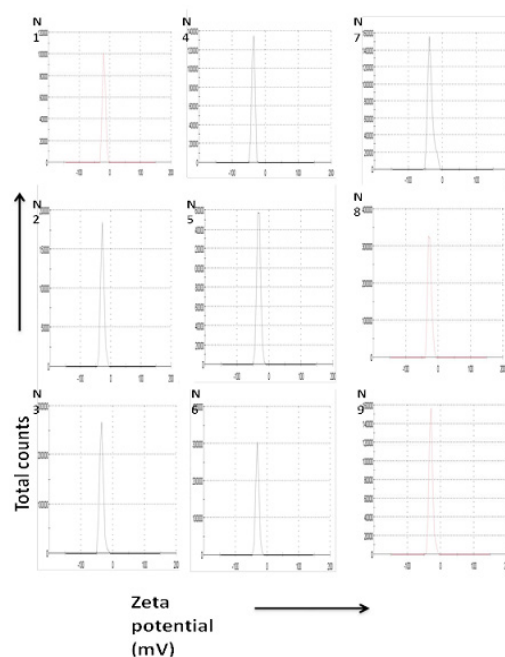


Figure 2. Zeta Potential of Synthesized PEG-Based Nanoparticles

Table 3. The Best Docking Score and Binding Energy of Compounds Docked Into PTK, and the Distances and Angles of Hydrogen Bonds between Compounds and Amino Acids Involved in PTK

Compound	C-DOCKER Interaction energy (kcal/mol)	Binding energy (kcal/mol)	Hydrogen bonds between compounds and amino acid			RMSD (Å°)
			Atom of comp	amino acid	distance	
1	47.3	18	Ar-OCH ₃	Lue813	1.92	0.66
2	41.2	20	Ar-OCH ₃	Lue813	2.12	1.02
3	44.7	16	Ar-OCH ₃ NH	Lue813 His790	1.95 2.01	0.75
4	44.5	21	Ar-OCH ₃	Phe811	2.16	0.88
5	-	-	-	-	-	--
6	45.5	19	NH N	Cys788 Ile789	2.43	0.32
7	46.3	21	N	Cys788	2.01	0.75
8	40.2	24	-	-	1.89	1.25
9	45.1	17	Pyrazole NH	Cys788	2.25	1.02

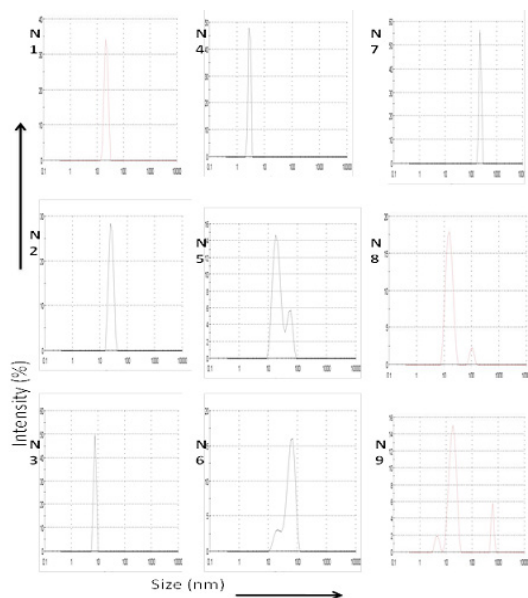


Figure 3. Particle Size Distribution of Synthesized PEG-Based Nanoparticles

structures.(c.f. Materials and Methods).

Characterization of PEG Nanoparticles

Particle size distribution and zeta potential of the synthesized drug nanoparticles are shown in Figures 2 and 3 and the data-values are summarized in Table 1. The formulation code of compound 1-9 are N1-N9 respectively, it appears that most of the particles having comparable sizes and less than 100 nm. The relatively changes in the sizes might be due to the nature of structure and composition of each drug derivative. The average particle size are 22.25, 25.9, 7.63, 2.85, 20.5, 60.9, 227.9, 15.79, 18.37 nm for N1, N2, N3, N4, N5, N6, N7, N8, N9, respectively. The results of zeta potential indicate the stability of the synthesized drug nanoparticles with the surface negative charges ranging between -19 to -36. The values and type of charges on the particle are depending on the composition and structure of the particle as well

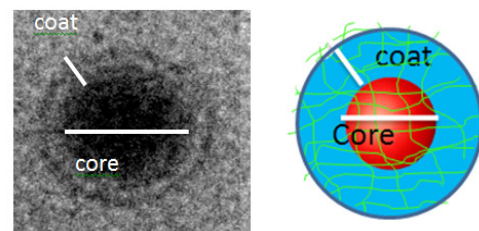


Figure 4. TEM Image of Synthesized Core-Shell PEG-Drug Nanoparticle

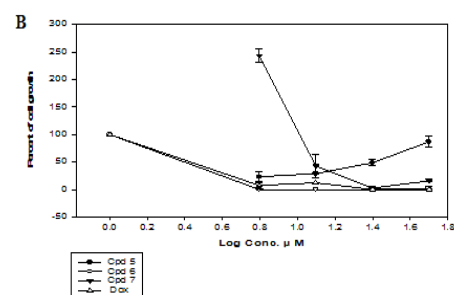
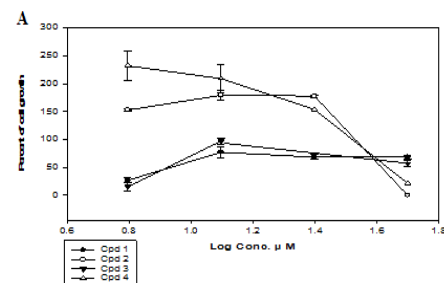


Figure 5 (A-B). Effect of PEG Based Nanoparticles Compounds (1-7) and Doxorubicin (Dox) on Hepg2 Cancer Cell Line Growth

as the medium in which the particles are suspended. The obtained values of zeta potential are -19.3, -27.4, -35.2, -35.8, -32.1, -30.5, -34.7, -26.2 and -28.8 mv for N1, N2, N3, N4, N5, N6, N7, N8 and N9, respectively.

Figure 4 depicts TEM image of the synthesized

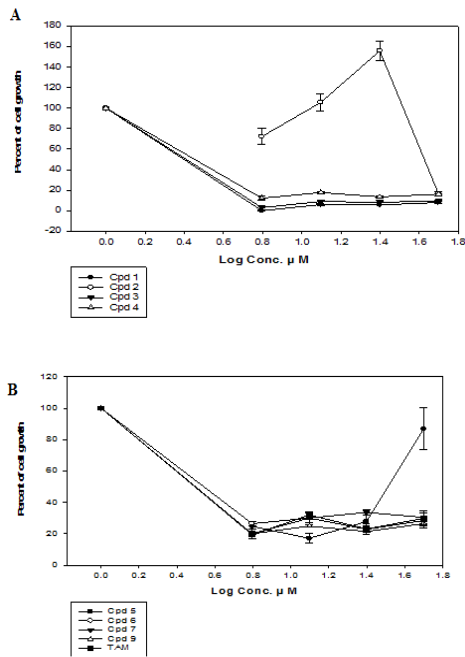


Figure 6 (A-B). Effect of PEG Based Nano Particles Compounds (1-9) and Tamoxifen (TAM) On MCF-7 Cancer Cell Line Growth

core-shell PEG-drug nanoparticles. Spherical drug nano particle coated with thin layer of PEG is appeared in the photograph. The core drug particle might be composed of several agglomerated nanoparticles.

The results of measured entrapped drug concentration by HPLC inside the synthesized core-shell nanoparticles after dialysis are illustrated in Table 1. The measured concentration values are 81.7, 760, 25.3, 633, 156.8, 348, 348, 0 and 867 $\mu\text{g/ml}$ for N1, N2, N3, N4, N5, N6, N7, N8 and N9, respectively. Big differences in the values of entrapped concentrations are detected. This might be depending on the structure and composition of each

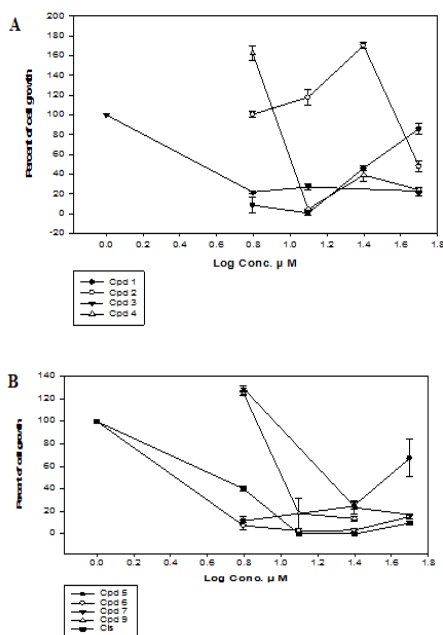


Figure 7. Effect of PEG Based Nano Particles Compounds (1-9) and Cisplatin (Cis) on HCT116 Cancer Cell Line

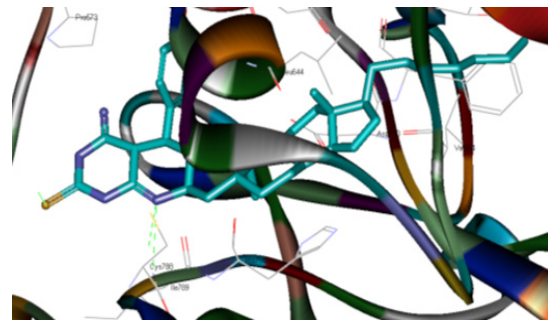
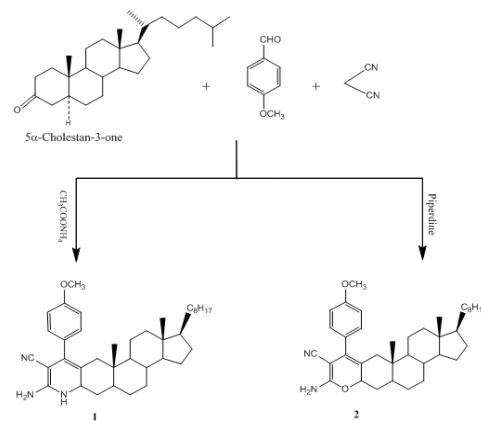


Figure 8. Docking Pose of the Target Compounds 6 to the Active Site of PTK which Exhibited Two Hydrogen Bond Shown as a Green Line with Amino Acid Cys 788 And Ile789.



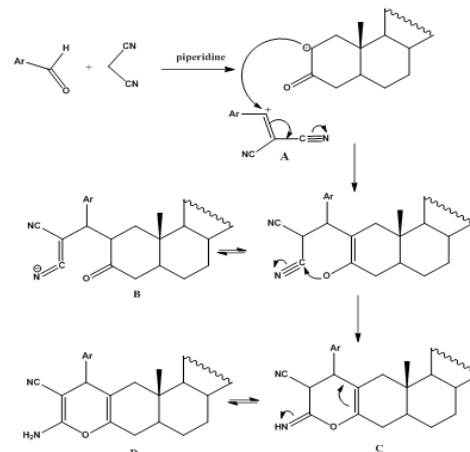
Scheme 1.

derivative.

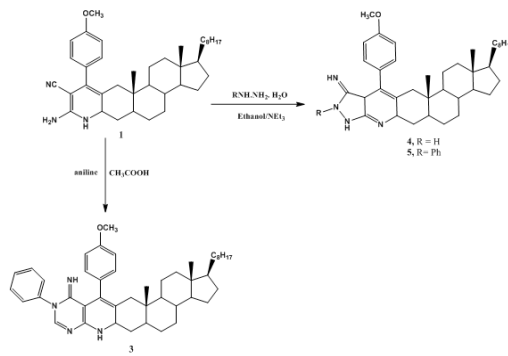
Cytotoxic Activity Assay

The newly synthesized compounds were investigated individually in their free and PEG based nano size form as anticancer agents against the three human cell lines namely, HepG2, MCF-7 and HCT116 at concentrations of (6.25, 12.5, 25, 50 $\mu\text{mol/l}$). The inhibition of proliferation of these cell line was determined using a neutral red assay, which is based on the ability of viable cells to incorporate and bind the supravital dye neutral red in the lysosomes.

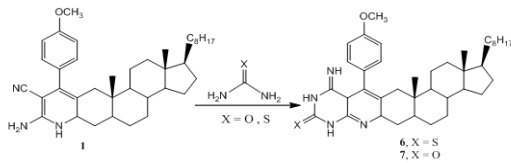
The free tested compounds, in normal size, did not



Scheme 2.



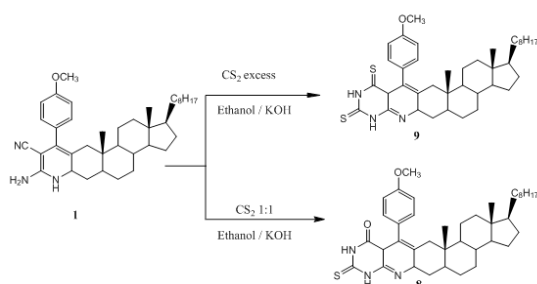
Scheme 3.



Scheme 4.

show significant effect on cell proliferation; however, their encapsulated nano-form affected significantly on cell growth inhibition as compared to the control cells. From the data obtained (Table 2, Figure 5), the tested compounds showed significant cell growth inhibition against HepG2 cells, the most active compounds were in the descending order of 6>3>1>7>5>2>4>9. Doxorubicin was used as a reference drug (IC_{50} , 2.63 $\mu\text{mol/l}$). Regarding MCF-7 cells where tamoxifen was used as a reference drug (IC_{50} , 3.09 $\mu\text{mol/l}$), as shown in Table 2 and Figure 6, the most active compounds against the MCF-7 were in the descending order of 1>3>4>9>7>6>5>2. Concerning HCT116 cells, where cisplatin was used as a reference drug (IC_{50} 4.67 $\mu\text{mol/l}$), the most active compounds against the HCT116 cancer cell line were in the descending order of 6>3>9>4<7>1>5>2 (Table 2, Figure 7).

The existence of [1,2-g] pyrimido [4,5-b] quinoline-9(2H)-thione at position 5 and 6 of naphthalene ring at compound 6 showed growth inhibition with IC_{50} values of 2.44 $\mu\text{mol/l}$, 3.46 $\mu\text{mol/l}$ and 2.59 $\mu\text{mol/l}$ against the three tested cell lines HepG2, MCF-7 and HCT116 respectively. Whereas, the existence of pyridine ring incorporated to compound 1 showed IC_{50} value of 2.45 $\mu\text{mol/l}$ against MCF-7 cells.



Scheme 5.

Discussion

Molecular Docking Study

The synthesized hybrid compounds are composed of two parts, due to the existence of bulky lipophilic cholestane moiety, the main interaction enrolled in the docking simulation was van der Waals forces, most of the compounds displayed only one hydrogen bonding with the PTK receptor Table 3. Almost all compounds showed similar binding affinities when compared with the native bound STI-571 ligand. The affinity of these hybrid compounds could be related to the high lipophilicity of the steroid moiety of the compound, due to which better van der Waals interaction was proposed between the receptor and ligand. Compound 6 in its PEG based nano size revealed the best cytotoxic effect against HepG2 and HCT116 cell lines with IC_{50} 2.44 $\mu\text{mol/l}$ and 2.59 $\mu\text{mol/l}$, respectively. Besides it showed a considerable low IC_{50} value against MCF-7 (3.46 $\mu\text{mol/l}$). Regarding the docking study it exhibited two hydrogen bonds with Cys788 and Ile789 showed C-DOCKER Interaction energy= 45.5 kcal/mol) with RMSD= 0.32 Figure 8. Consequently, the docking results were confirmed by the laboratory cytotoxic studies in Table 2.

In conclusion, this study introduced a facile synthesis of newly promising anticancer hybrid steroid derivatives via MCRs, and emphasized also the importance of converting heterocyclic steroids into PEG-based nanoparticles to form new effective anticancer agents. Compound 6 in its PEG based nano size revealed the best cytotoxic effect against HepG2 and HCT116 cell lines. Besides it showed a considerable low IC_{50} value against MCF-7. Finally, we recommend these heterocyclic steroidal nanoparticles as target for extension studies before going through phase 1 of clinical trials.

Abbreviations

NP, Nanoparticles; SAR, structure-activity relationship; MCRs, Multicomponent reactions; PEG, polyethylene glycol; WHO, world health organization; RES, Reticuloendothelial system; EPR, permeability and retention effect; TLC, thin layer chromatography; SDS, sodium dodecyl sulfate; SCMC, sodium carboxymethyl cellulose; SCMD, sodium carboxymethyl dextran; EE, entrapment efficiency; HPLC, High performance liquid chromatography; MWCO, Molecular weight cut-off; TEM, Transmission Electron Microscope; PCS, Photon correlation spectroscopy; ATCC, American Type Culture Collection; FBS, fetal bovine serum; DPBS, Dulbecco's phosphate-buffered saline; DMSO, Dimethyl sulfoxide; PTK, protein tyrosine kinase; DLS, Dynamic Light Scattering; EDTA, Ethylene diaminetetraacetic acid; TAM, Tamoxifen; Cis, Cisplatin; Dox, Doxorubicin.

Acknowledgments

The authors acknowledge the financial support of the National Research Centre, Cairo, Egypt, Project no: 10010105 (2014-2016), Granted for Prof. Gamal A Elmegeed.

References

- Discovery studio 2.0. Accelrys (2003), Inc., San Diego, CA.
- Dubey R, Oparil S, Imthurn B, Jackson E (2002). Sex hormones and hypertension. *Cardiovasc Res*, **53**, 688–708.
- Dueland S, Pedersen JI, Drevon CA, Bjorkhem I (1982). 26-Hydroxylation of SP-cholestane-3 α ,7 α , 12 α -triol by isolated nonparenchymal cells and hepatocytes from rat liver. *J lipid Res*, **23**, 1321-7.
- El-Far M, Elmegeed GA, Eskander EF, Rady HM, Tantawy MA (2009). Novel modified steroid derivatives of androstanolone as chemotherapeutic anti-cancer agents. *Eur J Med Chem*, **44**, 3936-46.
- Elmegeed GA, Khalil WB, Mohareb RM, et al (2011). Cytotoxicity and gene expression profiles of novel synthesized steroid derivatives as chemotherapeutic anti-breast cancer agents. *Bioorg Med Chem*, **19**, 6860-72.
- Elmegeed GA, Ahmed HH, Hashash MA, Abd-Elhalim MM, El-kady DS (2015). Synthesis of novel steroidal curcumin derivatives as anti-Alzheimer's disease candidates: Evidences-based on in vivo study. *Steroids*, **101**, 78-89.
- Elmegeed GA, Ahmed HH, Hussein JS (2005). Novel synthesized aminosteroidal heterocycles intervention for inhibiting iron-induced oxidative stress. *Eur J Med Chem*, **40**, 1283-94.
- Gacs-Baitz E, Minuti L, Taticchi A (1996). Synthesis and complete ¹H and ¹³C NMR analysis of some 4-androsten-3-one derivatives. *Synop*, **27**, 324–5.
- Ghosh D, Ghosh S, Sarkar S, et al (2010). Quercetin in vesicular delivery systems: Evaluation in combating arsenic induced acute liver toxicity associated gene expression in rat model. *Chem. Biol Interact*, **186**, 61–71.
- Gower B, Makin H (1984). Biochemistry of steroid hormones. Oxford/ London/Edinburgh: Blackwell Scientific Publications, pp 122.
- Hanahan D, Weinberg R (2000). The hallmarks of cancer. *Cell*, **100**, 57-70.
- Johnson LN, De Molinera E, Brown NR, et al (2002). Structural studies with inhibitors of the cell cycle regulatory kinase cyclin-dependent protein kinase 2. *Pharmacol Ther*, **93**, 113-24.
- Lammers T, Hennink WE, Storm G (2008). Tumor targeted nanomedicines: principles and practice. *Br J Cancer*, **99**, 392–7.
- Latham K, Zamora A, Drought H, et al (2003). Estradiol treatment redirects the isotype of the autoantibody response and prevents the development of autoimmune arthritis. *J Immunol*, **171**, 5820–07.
- Mohareb RM, Megally Abdo NY, Mohamed AA (2016). Cytotoxicity and anti-proliferative properties of heterocyclic compounds derived from progesterone. *Anticancer Agents Med Chem*, **16**, 1043-54.
- Repetto G, Peso AD, Zurita JL (2008). Neutral red uptake assay for the estimation of cell viability/cytotoxicity. *Nat Prot*, **3**, 1125–31.
- Sheridan PJ, Blum K, Trachtenberg M (1988). Steroid receptors and disease. New York: Marcel Dekker, pp 289–564.
- Shrestha AR, Shindo T, Ashida N, Nagamatsu T (2008). Synthesis, biological active molecular design, and molecular docking study of novel deazaflavin–cholestane hybrid compounds. *Bioorg Med Chem*, **16**, 8685–96.
- Singh H, Jindal DP, Yadav MR, Kumar M (1991). Heterosteroids and drug research. *Med Chem*, **28**, 233-315.
- Tan JS, Butterfield DE, Voycheck CL, Caldwell KD, Li JT (1993). Surface modification of nanoparticles by PEO/PPO block copolymers to minimize interactions with blood components and prolong blood circulation in rats. *Biomaterials*, **14**, 823-33.
- Vaculikova E, Grunwaldova V, Kral V, Dohnal J, Jampilek J (2012). Primary investigation of the preparation of nanoparticles by precipitation. *Molecules*, **17**, 11067-78.
- Váradi A, Palmer TC, NotisDardashti R, Majumdar S (2016). Isocyanide-based multicomponent reactions for the synthesis of heterocycles. *Molecules*, **21**, 1-22.
- Vulpetti A, Casale E, Roletto F, et al (2005). Structure-based drug design to the discovery of new 2-aminothiazole CDK2 inhibitors. *J Mol Graph Model*, **24**, 341-8.
- Wu TH, Yang RL, Xie LP, et al (2006). Inhibition of cell growth and induction of G1-phase cell cycle arrest in hepatoma cells by steroid extract from meretrix. *Cancer Lett*, **232**, 199–205.
- World Health Organization. www.who.int/mediacenter/factsheets/fs297/en/.
- Zhang BL, Zhang E, Pang, LP, et al (2013). Design and synthesis of novel D-ring fused steroidal heterocycles. *Steroids*, **78**, 1200-8.